Technical report 14-005

Optimal trajectory planning for trains under fixed and moving signaling systems using mixed integer linear programming*

Y. Wang, B. De Schutter, T.J.J. van den Boom, and B. Ning

Optimal Trajectory Planning for Trains under Fixed and Moving Signaling Systems Using Mixed Integer Linear Programming

Yihui Wang[a,b,*], Bart De Schutter[a], Ton J.J. van den Boom[a], Bin Ning[b]

[a]*Delft Center for Systems and Control, Delft University of Technology, 2628 CD Delft, The Netherlands*
[b]*State Key Laboratory of Rail Traffic Control and Safety, Beijing Jiaotong University, Beijing 100044, P.R. China*

Abstract

The optimal trajectory planning problem for multiple trains under fixed block signaling systems and moving block signaling systems is considered. Two approaches are proposed to solve this optimal control problem for multiple trains: the greedy approach and the simultaneous approach. In each solution approach, the trajectory planning problem is transformed into a mixed integer linear programming (MILP) problem. In particular, the objective function considered is the energy consumption of trains and the nonlinear train model is approximated by a piece-wise affine model. The varying line resistance, variable speed restrictions, and maximum traction force, etc. are also included in the problem definition. In addition, the constraints caused by the leading train in a fixed or moving block signaling system are first discretized and then transformed into linear constraints using piecewise affine approximations resulting in an MILP problem. Simulation results comparing the greedy MILP approach with the simultaneous MILP approach show that the simultaneous MILP approach yields a better control performance but requires a higher computation time. Moreover, the performance of the proposed greedy and the proposed simultaneous MILP approach is also compared with that of the greedy and the simultaneous pseudospectral method, where the pseudospectral method is a state-of-the-art method for solving optimal control problems. The results show that the energy consumption and the end time violations of the greedy MILP approach are slightly larger than those of the greedy pseudospectral method, but the computation time is one to two orders of magnitude smaller. The same trend holds for the simultaneous MILP approach and the simultaneous pseudospectral method.

Keywords: trajectory planning, train operation, signaling system, MILP, pseudospectral

1. Introduction

Nowadays, the energy efficiency of transportation systems is becoming more and more important because of the rising energy prices and environmental concerns. Rail traffic plays a significant role for the sustainability for transportation systems, since it can provide safe, fast, punctual, and comfortable services (Peng, 2008). The reduction of energy consumption is one

---

*Corresponding author. Tel:+31 1527 82725; Fax:+31 1527 86679.
Email addresses: yihui.wang@tudelft.nl (Yihui Wang), b.deschutter@tudelft.nl (Bart De Schutter), a.j.j.vandenboom@tudelft.nl (Ton J.J. van den Boom), bning@bjtu.edu.cn (Bin Ning)

of the key objectives of railway systems because energy consumption is one of the major expenses in operational cost, which is about 13% - 16% of the annual operation and maintenance cost of railway systems in China (Ding et al., 2009). Therefore, even a small improvement in energy saving is attractive to the railway operators since it can save a large amount of money. Some driver assistance systems have been developed to assist drivers to drive the train optimally, such as FreightMiser (Howlett & Pudney, 1995), Metromiser (Howlett & Pudney, 1995), and driving style manager (Franke et al., 2002). With the development of modern railway systems, an automatic train operation system plays a key role in ensuring accurate stopping, operation punctuality, energy saving, and riding comfort (Peng, 2008). The railway control center or automatic train operation systems are responsible for solving the trajectory planning problems based on the information collected by train monitoring systems, such as line resistance, speed limits, maximum traction and braking forces.

In the literature, the research on the optimal control of train operations began in the 1960s and is aimed at solving the trajectory planning problem for a train running from one station to another. Since it has significant effects for energy saving, punctuality, etc., various approaches were proposed for the trajectory planning problem. These approaches can be grouped into two main categories: analytical solutions and numerical optimization. For analytical solutions, the maximum principle is applied and it results in four optimal regimes (i.e., maximum traction, cruising, coasting, and maximum braking) (Howlett et al., 1994; Howlett, 2000; Khmelnitsky, 2000; Liu & Golovicher, 2003). It is difficult to obtain the analytical solution if more realistic conditions are considered as these introduce more complex nonlinear terms into the model equations and the constraints (Ko et al., 2004). Numerical optimization approaches are applied more and more to the train optimal control problem due to the increasing computing power nowadays. A number of advanced techniques such as fuzzy and genetic algorithms have been proposed to calculate the optimal reference trajectory for trains, see e.g. Chang & Xu (2000); Chang & Sim (1997); Han et al. (1999); Ke et al. (2011). But in these approaches, the optimal solution is not always guaranteed to be found. On the other hand, multi-parametric quadratic programming is used in (Vašak et al., 2009) to calculate the optimal control law for train operations. In that approach, the nonlinear train model with quadratic resistance is approximated by a piecewise affine function. Inspired by (Vašak et al., 2009), in Wang et al. (2011, 2013) we proposed to solve the optimal trajectory problem as a mixed integer linear programming (MILP) problem, which can be solved efficiently using existing commercial and free solvers (Linderoth & Ralphs, 2005; Atamtürk & Savelsbergh, 2005) that guarantee finding the global optimum of the MILP problem.

However, the approaches mentioned above ignore the impact caused by the signaling systems, e.g., a fixed block signaling (FBS) system or a moving block signaling (MBS) system. An FBS system is a block system using fixed block sections, which are protected by trackside traffic signals. A train cannot enter a block section until a signal indicates the train may proceed. In an MBS system, the blocks are defined as safe zones around each train in real time. Regular communication between trains and zone controllers is needed for knowing the exact locations and speeds of all trains in that zone at any given time. An MBS system allows trains to run closer together compared with an FBS system, thus increasing the line capacity. Lu & Feng (2011) consider the operation of two trains on a same line and optimize the trajectory of the following train with constraints caused by the leading train in an FBS system. More specifically, a parallel genetic algorithm is used to optimize the trajectories for the leading train and the following train, resulting in a lower energy consumption (Lu & Feng, 2011). Gu et al. (2011) apply nonlinear programming to optimize the trajectory for the following train. Two situations of the leading train, i.e. running and stopped, are studied and the corresponding strategies are proposed for the

following train. In addition, Ding et al. (2009) take the constraints caused by the MBS system into account and develop an energy-efficient multi-train control algorithm to calculate the optimal trajectories. Three optimal control regimes, i.e. maximum traction, coasting, and maximum braking, are adopted in the algorithm and the sequences of these three regimes are determined by a predefined logic.

In this paper, the constraints caused by the leading train in an FBS system and an MBS system are formulated. These constraints are discretized and then recast as linear constraints by piecewise affine approximations. Thus, they can be easily included into the MILP problem, which can be solved efficiently compared to the existing approaches. Furthermore, the greedy approach and the simultaneous approach are proposed to solve the trajectory planning problem for multiple trains. We also compare the MILP approach with the state-of-art optimization approach: pseudospectral methods. Over the last decade, pseudospectral methods have risen to prominence in the numerical optimal control area (Elnagar et al., 1995), which were applied to solving optimal control problems (Gong et al., 2007), such as orbit transfers, lunar guidance, magnetic control. Therefore, we have selected the pseudospectral method for the comparison of the case study.

The remainder of this paper is structured as follows. In Section 2, the train model and the MILP approach for a single train are summarized based on Wang et al. (2013). Section 3 introduces the principle of railway signaling systems, i.e. the FBS system and the MBS system. Section 4 formulates the constraints for the following train caused by the leading train under an FBS system and shows how to include these constraints into the MILP formulation. The constraints caused by the MBS system are considered and included in the MILP problem in Section 5. Section 6 illustrates the calculation of the optimal trajectories using the data from Beijing Yizhuang subway line. We conclude with a short discussion of some topics for future work in Section 7.

2. Train model and the MILP approach

In this section, the formulation of the optimal control problem and the MILP approach we proposed in Wang et al. (2013) are summarized.

2.1. Optimal control problem

A continuous-space mass-point model is often used in the literature on train optimal control (Franke et al., 2003), which can be described as follows (Liu & Golovicher, 2003):

$$
\begin{aligned}
m\rho \frac{\mathrm{d}\tilde{E}}{\mathrm{d}s} &= u(s) - R_{\mathrm{b}}(v) - R_{\mathrm{l}}(s, v), \\
\frac{\mathrm{d}\tilde{t}}{\mathrm{d}s} &= \frac{1}{\sqrt{2\tilde{E}}},
\end{aligned}
\tag{1}
$$

where m is the mass of the train, ρ is a factor to consider the rotating mass (Hansen & Pachl, 2008), $\tilde{E}$ is the kinetic energy per mass unit, which is equal to $0.5v^2$, v is the velocity of the train, s is the position of the train, u is the control variable, i.e. the traction or braking force, which is bounded by the maximum traction force $u_{\max}$ and the maximum braking force $u_{\min}$, so $u_{\min} \leq u(s) \leq u_{\max}$, $R_{\mathrm{b}}(v)$ is the basic resistance including roll resistance and air resistance, and $R_{\mathrm{l}}(s, v)$ is the line resistance caused by track grade, curves, and tunnels. See Wang et al. (2013) for more details.

3

The kinetic energy per mass unit $\tilde{E} = 0.5v^2$ and time t are chosen as the states and the position s is taken as the independent variable for the train model as in (Franke et al., 2003). The trajectory planning problem for trains can then be formulated as (Wang et al., 2011):

$$J = \int_{s_{\text{start}}}^{s_{\text{end}}} \max\left(0, u(s)\right) \mathrm{d}s \tag{2}$$

subject to

$$\begin{aligned}
&u_{\min} \leq u(s) \leq u_{\max}, \\
&0 < \tilde{E}(s) \leq \tilde{E}_{\max}(s), \\
&\tilde{E}(s_{\text{start}}) = \tilde{E}_{\text{start}}, \quad \tilde{E}(s_{\text{end}}) = \tilde{E}_{\text{end}}, \\
&t(s_{\text{start}}) = 0, \quad t(s_{\text{end}}) = T,
\end{aligned} \tag{3}$$

and the train model (1), where the objective function J is the energy consumption without regenerative braking; $\tilde{E}_{\max}(s)$ is equal to $0.5V_{\max}^2(s)$ where $V_{\max}(s)$ is the maximum allowable velocity, which depends on the train characteristics and line conditions, and as such it is usually a piecewise constant function of the coordinate s (Khmelnitsky, 2000; Liu & Golovicher, 2003); s_{start}, $\tilde{E}(s_{\text{start}})$, and $t(s_{\text{start}})$ are the position, the kinetic energy per mass, and the departure time at the beginning of the route; s_{end}, $\tilde{E}(s_{\text{end}})$, and $t(s_{\text{end}})$ are the position, the kinetic energy per mass, and the arrival time at the end of the route, where the scheduled running time T is given by the timetable or the rescheduling process. It is assumed that the unit kinetic energy $\tilde{E}(s) > 0$, which means the train's speed is always strictly larger than zero, i.e. the train travels nonstop (Khmelnitsky, 2000). This assumption is nonrestrictive in practice because the initial start and terminal stop can be modeled by small nonzero velocities. Furthermore, in principle the traffic management system does not plan stops intentionally at an intermediate point of the trip.

2.2. Transformation properties

The transformation properties given by Williams (1999) (see (4)-(7) below) will be used to reformulate the nonlinear optimal control problem as an MILP problem. More specifically, first, the nonlinear train model (1) is transformed into a mixed logical dynamic model. Next, the nonlinear constraints in the optimal control problem for the mixed logical dynamic model are approximated using piecewise functions and written as mixed integer linear constraints. This results in an MILP problem.

Consider the statement $\tilde{f}(\tilde{x}) \leq 0$, where $\tilde{f} : \mathbb{R}^n \to \mathbb{R}$ is affine, $\tilde{x} \in \chi$ with $\chi \subset \mathbb{R}^n$ and let

$$\tilde{M} = \max_{\tilde{x} \in \chi} \tilde{f}(\tilde{x}), \quad \tilde{m} = \min_{\tilde{x} \in \chi} \tilde{f}(\tilde{x}). \tag{4}$$

If we introduce the logical variable $\delta \in \{0, 1\}$, then the following equivalence holds:

$$[\tilde{f}(\tilde{x}) \leq 0] \Leftrightarrow [\delta = 1] \quad \text{is true iff} \quad \begin{cases} \tilde{f}(\tilde{x}) \leq \tilde{M}(1 - \delta) \\ \tilde{f}(\tilde{x}) \geq \varepsilon + (\tilde{m} - \varepsilon)\delta \end{cases} \tag{5}$$

where ε is a small positive number (typically the machine precision) that is introduced to transform a strict equality into a non-strict inequality, which fits the MILP framework (Bemporad & Morari, 1999).

The product of two logical variables $\delta_1 \delta_2$ can be replaced by an auxiliary logical variable $\delta_3 = \delta_1 \delta_2$, i.e. $[\delta_3 = 1] \leftrightarrow [\delta_1 = 1] \wedge [\delta_2 = 1]$, which is equivalent to

$$\begin{cases} -\delta_1 + \delta_3 \leq 0, \\ -\delta_2 + \delta_3 \leq 0, \\ \delta_1 + \delta_2 - \delta_3 \leq 1. \end{cases} \tag{6}$$

Moreover, the product $\delta \tilde{f}(\tilde{x})$ can be replaced by the auxiliary real variable $z = \delta \tilde{f}(\tilde{x})$, which satisfies $[\delta = 0] \Rightarrow [z = 0]$ and $[\delta = 1] \Rightarrow [z = \tilde{f}(\tilde{x})]$. Then $z = \delta \tilde{f}(\tilde{x})$ is equivalent to

$$\begin{cases} z \leq \tilde{M}\delta, \\ z \geq \tilde{m}\delta, \\ z \leq \tilde{f}(\tilde{x}) - \tilde{m}(1 - \delta), \\ z \geq \tilde{f}(\tilde{x}) - \tilde{M}(1 - \delta). \end{cases} \tag{7}$$

It is noted that (5), (6), and (7) yield linear inequalities since $\tilde{f}$ is affine.

2.3. The mixed integer linear programming (MILP) approach

In Wang et al. (2011), the continuous-space model (1) of train operations has been discretized in space: the position horizon between two stations without intermediate station $[s_{\text{start}}, s_{\text{end}}]$ is split into N intervals and it is assumed that the track and train parameters as well as the traction or the breaking force can be considered as constant in each interval $[s_k, s_{k+1}]$ with length $\Delta s_k = s_{k+1} - s_k$, for $k = 1, 2, \ldots, N$. The discrete-space model is then transcribed into a piecewise affine (PWA) model by approximating the nonlinear terms through PWA functions. Furthermore, by applying the transformation properties described in Section 2.2, the PWA model is formulated as the following mixed logical dynamic model (see Wang et al. (2011)):

$$x(k+1) = A_k x(k) + B_k u(k) + C_{1,k}\delta(k) + C_{2,k}\delta(k+1) + D_{1,k}z(k) + D_{2,k}z(k+1) + e_k, \tag{8}$$

$$R_{1,k}\delta(k) + R_{2,k}\delta(k+1) + R_{3,k}z(k) + R_{4,k}z(k+1) \leq R_{5,k}u(k) + R_{6,k}x(k) + R_{7,k}, \tag{9}$$

where $x(k) = \begin{bmatrix} E(k) & t(k) \end{bmatrix}^T$, $\delta(\cdot)$ and $z(\cdot)$ contain the binary variables and auxiliary variables introduced by the transformation properties, and (9) also includes the upper bound and lower bound constraints for $E(k)$, $t(k)$, and $u(k)$. For the sake of simplicity, we use $E(k)$ and $t(k)$ as a short-hand notation for $\tilde{E}(s_k)$ and $\tilde{t}(s_k)$, respectively. The coefficient matrices in the mixed logical dynamic model are determined by the train model, the PWA approximations, upper bounds and lower bound constraints, etc.

The objective of the trajectory planning problem is considered as the energy consumption of the train operation without regenerative braking, which can be described as

$$J = \sum_{k=1}^{N} \max(0, u(k))\Delta s_k. \tag{10}$$

As shown in Wang et al. (2011), the optimal control problem can be recast as the following mixed integer linear programming (MILP) problem by introducing a new auxiliary variable $\omega(k)$ to deal with the function $\max(0, u(k))$ in the objective function (10):

$$\min_{\tilde{V}} \quad C_J^T \tilde{V}, \tag{11}$$

5

subject to

$$F_1 \tilde{V} \leq F_2 x(1) + f_3$$
$$F_4 \tilde{V} = F_5 x(1) + f_6$$

(12)

where $C_J = \begin{bmatrix} 0 & \cdots & 0 & \Delta s_1 & \cdots & \Delta s_N \end{bmatrix}^T$, $\tilde{V} = \begin{bmatrix} \tilde{u}^T & \tilde{\delta}^T & \tilde{z}^T & \tilde{\omega}^T \end{bmatrix}^T$,

$$\tilde{u} = \begin{bmatrix} u(1) \\ u(2) \\ \vdots \\ u(N) \end{bmatrix}, \tilde{\delta} = \begin{bmatrix} \delta(1) \\ \delta(2) \\ \vdots \\ \delta(N+1) \end{bmatrix}, \tilde{z} = \begin{bmatrix} z(1) \\ z(2) \\ \vdots \\ z(N+1) \end{bmatrix}, \tilde{\omega} = \begin{bmatrix} \omega(1) \\ \omega(2) \\ \vdots \\ \omega(N+1) \end{bmatrix},$$

for properly defined matrices and vectors F_1, F_2, f_3, F_4, F_5, and f_6. The MILP problem (11)-(12) can be solved by several existing commercial and free solvers, such as CPLEX, Xpress-MP, GLPK (see e.g. Linderoth & Ralphs (2005); Atamtürk & Savelsbergh (2005)).

3. Principle of block signaling systems

Block signaling is used to maintain a safe distance between successive trains on the same track. The main principles of the fixed block signaling system and the moving block signaling system are presented next.

3.1. Fixed block signaling system

The fixed blocking signaling (FBS) system is commonly used in the railway operation systems nowadays (Pachl, 2009). In FBS system, the line is divided into blocks, the length of which depends on the maximum train speed, the worst-case braking rate, and the number of signal aspects, which mark the visual appearance of the signal, such as a green, yellow, or red light. Each block is exclusively occupied by only one train and the presence of a train within a block is usually detected by the track circuits (Takeuchi et al., 2003). Furthermore, the blocks are protected by lineside or cab signals. Lineside signals are still typical in railways, however, cab signals are used more and more, in particular on high-speed lines where lineside signals cannot be watched clearly by the driver because of the high speed. There exist two kinds of FBS systems, namely one-block signaling and multiple-block signaling (Pachl, 2009). In one-block signaling, the indication of the block signal depends only on the state of the block section beyond the signal and every block signal must have a distant signal which is supposed to provide the required approach information. In multiple-block signaling systems, the indication of a block signal depends on the state of two or more following block sections. A simple example is a two-block signaling system with three aspects, i.e. red, yellow, and green, and which is called the three-aspect signaling system. Later on, we will discuss the constraints caused by fixed block signaling system using this simple three-aspect signaling system. However, the methodology proposed in this paper can be extended to other types of FBS systems.

A three-aspect signaling system is shown as Figure 1. On a line equipped with an automatic train protection system, each block carries an electronic speed code on top of its track circuit. The speed code data consists of two parts, the authorized-speed code for this block and the target-speed code for the next block. The speed code data is coded by the electronic equipment controlling the track circuitry and transmitted via the tracks. Then this speed code data is picked up by antennae on the train. If the train tries to enter a zero speed block or an occupied block, or if it enters a section at a speed higher than that authorized by the speed code, the on-board
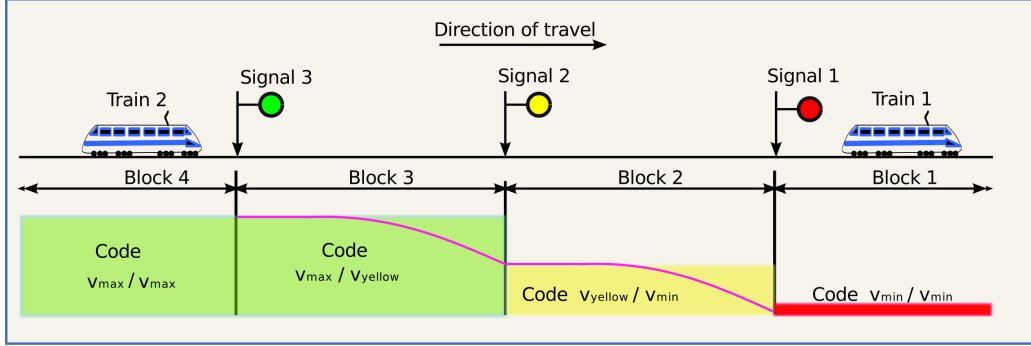
Figure 1: Speed codes for the fixed-block system

electronics will cause an emergency brake application. Figure 1 shows how the speed code works. When a train in Block 4 approaching to Signal 3 will receive a $v_{\max}/v_{\text{yellow}}$ code, to indicate a permitted speed of $v_{\max}$ in this block and a target speed of v_{yellow} for the next. When the train enters Block 2, the code changes to $v_{\text{yellow}}/v_{\min}$ because the next block (Block 1) is occupied by train 1, so the speed must be $v_{\min}$ (usually taking the value zero) by the time train reaches the end of Block 2. If the train attempts to enter Block 1, the on-board equipment will detect the minimum speed code ($v_{\min}/v_{\min}$) and will cause an emergency brake application.

In order to ensure that a train's operation is not impeded by the signaling system, i.e. a train's operation is not then affected by the train in front, the minimum headway is introduced. The minimum headway is the minimum time separation between successive trains at train stations. For undisturbed running In FBS system, the minimum headway can be defined as (Hill & Bond, 1995)

$$H_{\min,\text{FBS}} = \frac{L_a}{v_{\max}}\left[2 + \text{INT}\left\{\frac{L_r^F + (v_{\max}^F)^2/(2a_b^F)}{L_a}\right\}\right] + \frac{v_{\max}^F}{2a_b^F} + t_d^L + \sqrt{\frac{2(L_t^L + L_s)}{a_{\text{acc}}^L}}, \qquad (13)$$

where the L_a is the block length, L_r^F is the distance that the following train will travel during the reaction time t_r^F of the driver and/or train control equipment of the following train, $v_{\max}^F$ is the maximum speed of the following train, a_b^F is the maximum braking rate, t_d^L is the station dwell time of the leading train, L_t^L is the length of the leading train, L_s is the length of the secure section, and a_{acc}^L is the acceleration of the leading train.

3.2. Moving block signaling system

With the increasing operational density in railway systems, there is a shortage of transportation capacity for railway systems with an FBS system. Even though the line capacity of an FBS system can be increased using shorter block lengths, the installation and maintenance cost of the signaling and track equipment may not be justified by the increasing capacity. Consequently, moving block signaling (MBS) systems have been proposed to achieve even higher performance.

An MBS system relies on the continuous bidirectional communication connections between trains and zone controllers. A zone controller calculates the limit-of-movement-authority for every train in the zone it controls and makes sure that trains will be running with a safe distance with respect to other trains. More specifically, the limit-of-movement-authority indicates the tail
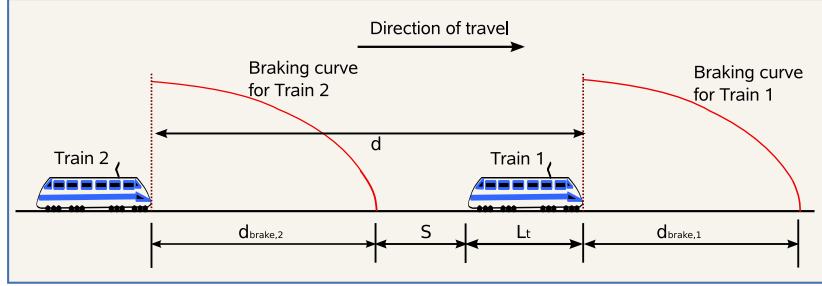
Figure 2: The principle of a pure MBS system

of the preceding train with a safety margin included, i.e. the maximum position that a train is allowed to move to. In addition, the limit-of-movement-authority of the following train moves forward continuously as the leading train travels. In the literature, four MBS schemes (Pearson, 1973) have been discussed: moving space block signaling, moving time block signaling, pure MBS, and relative MBS. Takeuchi et al. (2003) evaluated the first three schemes and compared them with the FBS scheme based on two basic criteria, namely steady state performance and perturbed performance. It is concluded that the pure MBS scheme gives the best performance. In addition, Takeuchi et al. (2003) stated that the concept of the relative MBS has never been accepted for normal rail traffic even though it is routinely accepted for road traffic. Therefore, we will consider the pure MBS scheme in this paper. However, the proposed approach can be extended to other MBS schemes too. Moreover, the pure MBS scheme is the basis of all systems currently implemented in practice (Takeuchi et al., 2003), the principle of which is shown in Figure 2.

In pure MBS system, the minimum distance between two successive trains is basically the instantaneous braking distance required by the following train plus a safety margin. Therefore, even if the leading train comes to a sudden halt, a collision can be avoided by using the minimum distance. In practice, the minimum distance in the MBS system is larger because the driver or the automatic train control system need time to react to situations. Furthermore, the train length has to be considered too. Therefore, the minimum distance of a practical MBS system is modified as (Takeuchi et al., 2003)

$$s^{\mathrm{L}}(t) - s^{\mathrm{F}}(t) \geq L_{\mathrm{r}}^{\mathrm{F}} + (v^{\mathrm{F}}(t))^2/(2a_{\mathrm{b}}^{\mathrm{F}}) + S_{\mathrm{SM}} + L_{\mathrm{t}}^{\mathrm{L}}, \tag{14}$$

where $s^{\mathrm{L}}(t)$ and $s^{\mathrm{F}}(t)$ are the positions of the front of the leading train and the following train at time t, $v^{\mathrm{F}}(t)$ is the speed of the following train, $a_{\mathrm{b}}^{\mathrm{F}}$ is the maximal braking rate, S_{SM} is the safety margin distance, $L_{\mathrm{r}}^{\mathrm{F}}$ is the distance that the following train will travel during the reaction time $t_{\mathrm{r}}^{\mathrm{F}}$ of the driver and/or train equipment of the following train, and $L_{\mathrm{t}}^{\mathrm{L}}$ is the length of the leading train. The value of the reaction time could be obtained from historical data. The minimum distance between two successive trains (14) can approximately[1] be recast as the minimum time difference of two successive trains

$$t^{\mathrm{F}}(s) - t^{\mathrm{L}}(s) \geq t_{\mathrm{r}}^{\mathrm{F}} + t_{\mathrm{b}}^{\mathrm{F}}(s) + t_{\mathrm{safe}}^{\mathrm{F}}(s), \tag{15}$$

---

[1]If $v^{\mathrm{F}}(t)$ is a constant, (15) is then exactly equivalent to (14).

8

where $t^L(s)$ and $t^F(s)$ are the time instants at which the front of the leading train and the following train pass position s, respectively. The braking time of the following train $t_b^F(s)$ and the time margin $t_{safe}^F(s)$ caused by the safe margin distance and the train length can be computed as

$$t_b^F(s) = v^F(s)/a_b^F, \tag{16}$$

$$t_{safe}^F(s) = (S_{SM} + L_t^L)/v^F(s), \tag{17}$$

where $v^F(s)$ is the speed of the following train at position s.

In order to ensure that near stations a train's operation is not impeded by the signaling system, i.e. a train's operation is not then affected by the (in principle slowly moving or stopped) train in front, the minimum headway is introduced. The minimum headway is the minimum time separation between successive trains at train stations, and it is defined as Takeuchi et al. (2003)

$$H_{min,MBS} = t_d^L + t_{in-out} = t_d^L + t_r^F + t_{b,max}^F + t_{safe}^L, \tag{18}$$

with the run-in/run-out time $t_{in-out} = t_r^F + t_{b,max}^F + t_{safe}^L$, where $t_{b,max}^F$ is the time it takes the following train to come to a full stop when it is running at its maximum speed, i.e. $t_{b,max}^F = v_{max}^F/a_b^F$, and the run-out time t_{safe}^L is the time that the leading train needs to completely clear the secure section (i.e. a special section to protect the leading train), if present, and including a safety margin, i.e.[2] $t_{safe}^L = \sqrt{2(S_{SM} + L_t^L + L_s)/a_{acc}^L}$. The acceleration of the leading train a_{acc}^L is usually considered as a constant value for the minimum headway calculation.

4. FBS system constraints and their formulation into the MILP approach

The constraints caused by the leading train in the FBS system are first discretized at each grid point s_k for $k = 1, 2, \cdots, N + 1$. These logical constraints are then transformed into linear constraints, which can be easily included in the MILP approach. Two solution approaches are proposed to solve the optimal control problem for multiple trains in FBS system.

4.1. Discretizing the FBS system constraints

We assume for each $m \in \{1, 2, \ldots, M\}$, there exists an index $l_m \in \{1, 2, \ldots, N+1\}$ such that

$$S_{FB,m} = s_{l_m}, \tag{19}$$

and define a piecewise constant function such that

$$\ell(k) = m, \quad \text{for} \quad l_m < k \le l_{m+1}, \quad \text{for} \quad m \in \{1, 2, \ldots, M\} \tag{20}$$

Then s_k is in the fixed block $(s_{l_{\ell(k)}}, s_{l_{\ell(k)+1}}]$. The constraints caused by the leading train in a three-aspect fixed block signaling system shown in Figure 1 can be transformed at each grid point s_k as the follows:

- If the following train and the leading train are in the same block section, i.e. $t^F(k) \in (t^L(l_{\ell(k)}), t^L(l_{\ell(k)+1})]$, which is in fact not allowed by signaling system, then the speed of the following train must equal to the minimum speed, i.e.

$$v^F(k) = V_{min}. \tag{21}$$

---

[2]The calculation of this time can be obtained using the equations given in the appendix.

- If the leading train is one block section before the following train, i.e. $t^{\text{F}}(k) \in \left(t^{\text{L}}(l_{\ell(k)+1}), t^{\text{L}}(l_{\ell(k)+2}) \right]$, then the speed of the following train at positions $s_{l_{\ell(k)}}$ and $s_{l_{\ell(k)+1}}$ should be less than or equal to V_{Yellow} and equal to V_{min}, respectively, i.e.

$$
\begin{aligned}
v^{\text{F}}_{l_{\ell(k)}} &\leq V_{\text{Yellow}}, \\
v^{\text{F}}_{l_{\ell(k)+1}} &= V_{\text{min}}.
\end{aligned}
\tag{22}
$$

The deceleration is assumed as a constant for the entire interval $[s_{l_{\ell(k)}}, s_{l_{\ell(k)+1}}]$. Based on the relationship among position, speed, and acceleration (see appendix), we have

$$
2a_{\ell(k)}\left(s_{l_{\ell(k)+1}} - s_{l_{\ell(k)}}\right) = V_{\text{min}}^2 - V_{\text{Yellow}}^2,
\tag{23}
$$

$$
2a_{\ell(k)}\left(s_k - s_{l_{\ell(k)}}\right) = \bar{V}_{\text{Yellow},k}^2 - V_{\text{Yellow}}^2,
\tag{24}
$$

where $a_{\ell(k)}$ is the deceleration and $\bar{V}_{\text{Yellow},k}$ is the maximum speed for trains at position s_k. By eliminating $a_{\ell(k)}$ in (23) and (24), we obtain

$$
\bar{V}_{\text{Yellow},k} = \sqrt{V_{\text{Yellow}}^2 + (V_{\text{min}}^2 - V_{\text{Yellow}}^2)\frac{s_k - s_{l_{\ell(k)}}}{s_{l_{\ell(k)+1}} - s_{l_{\ell(k)}}}},
\tag{25}
$$

which is a constant because all the elements in (25) are constants. Therefore, in this case we have the constraint

$$
v^{\text{F}}(k) \leq \bar{V}_{\text{Yellow},k}.
\tag{26}
$$

- If the leading train is two blocks before the following train, i.e. $t^{\text{F}}(k) \in \left(t^{\text{L}}(l_{\ell(k)+2}), t^{\text{L}}(l_{\ell(k)+3}) \right]$, then the speed of the following train at positions $s_{l_{\ell(k)}}$ and $s_{l_{\ell(k)+1}}$ should be less than or equal to V_{max} and V_{Yellow}, respectively, i.e.

$$
\begin{aligned}
v^{\text{F}}_{l_{\ell(k)}} &\leq V_{\text{max}}, \\
v^{\text{F}}_{l_{\ell(k)+1}} &\leq V_{\text{Yellow}}.
\end{aligned}
\tag{27}
$$

Similarly as $\bar{V}_{\text{Yellow},k}$, we can obtain

$$
\bar{V}_{\text{max},k} = \sqrt{V_{\text{max}}^2 + (V_{\text{Yellow}}^2 - V_{\text{max}}^2)\frac{s_k - s_{l_{\ell(k)}}}{s_{l_{\ell(k)+1}} - s_{l_{\ell(k)}}}},
\tag{28}
$$

where $\bar{V}_{\text{max},k}$ is the maximum speed for trains at position s_k. Note that $\bar{V}_{\text{max},k}$ is also a constant. Therefore, we in this case have the constraint

$$
v^{\text{F}}(k) \leq \bar{V}_{\text{max},k}.
\tag{29}
$$

4.2. Considering the FBS constraints into the MILP approach

In order to transform these logical constraints into linear constraints, the following binary variables are introduced:

$$
\begin{aligned}
[t^{\text{F}}(k) \leq t^{\text{L}}(l_{\ell(k)+1})] &\Leftrightarrow [\delta_1(k) = 1], \\
[t^{\text{F}}(k) \leq t^{\text{L}}(l_{\ell(k)+2})] &\Leftrightarrow [\delta_2(k) = 1], \\
[t^{\text{F}}(k) \leq t^{\text{L}}(l_{\ell(k)+3})] &\Leftrightarrow [\delta_3(k) = 1].
\end{aligned}
\tag{30}
$$

10

Note that an extra constraint is needed, i.e.

$$t^{\mathrm{F}}(k) > t^{\mathrm{L}}(k), \tag{31}$$

which means that the following train passes the position s_k later than the leading train in order to avoid the collision of trains. In addition, based on the definition of $\delta_1(k)$, $\delta_2(k)$, and $\delta_3(k)$, the following logical conditions are satisfied

$$\begin{aligned}
[\delta_1(k) = 1] &\Leftrightarrow [\delta_2(k) = \delta_3(k) = 1], \\
[\delta_2(k) = 1] &\Leftrightarrow [\delta_3(k) = 1].
\end{aligned} \tag{32}$$

The constraints caused by the leading train in the three-aspects fixed block signaling system can then be reformulated as:

$$\delta_1(k) v^{\mathrm{F}}(k) \leq V_{\min}, \tag{33}$$

$$(1 - \delta_1(k)) \delta_2(k) v^{\mathrm{F}}(k) \leq \bar{V}_{\mathrm{Yellow},k}, \tag{34}$$

$$(1 - \delta_2(k)) \delta_3(k) v^{\mathrm{F}}(k) \leq \bar{V}_{\max,k}, \tag{35}$$

where '$\leq$' is used in (33) because when $\delta_1(k) = 0$, $\delta_1(k) v^{\mathrm{F}}(k)$ is equal to 0, and not equal to $V_{\min}$.

By defining $\tilde{M}_i = T_{\max}^{\mathrm{F}} - t^{\mathrm{L}}(l_{\ell(k)+i}) \geq \max(t^{\mathrm{F}}(k) - t^{\mathrm{L}}(l_{\ell(k)+i}))$, $\tilde{m}_i = \min(t^{\mathrm{F}}(k) - t^{\mathrm{L}}(l_{\ell(k)+i})) \geq T_{\min}^{\mathrm{F}} - t^{\mathrm{L}}(l_{\ell(k)+i})$, the logical constraints (30) is equal to the following inequalities by transformation property (5):

$$\begin{aligned}
t^{\mathrm{F}}(k) - t^{\mathrm{L}}(l_{\ell(k)+i}) &\leq \tilde{M}_i(1 - \delta_i(k)), \\
t^{\mathrm{F}}(k) - t^{\mathrm{L}}(l_{\ell(k)+i}) &\geq \varepsilon + (\tilde{m}_i - \varepsilon)\delta_i(k),
\end{aligned} \tag{36}$$

for $i = 1, 2, 3$, where $T_{\max}^{\mathrm{F}}$ is the arrival time of the following train at the final destination, $T_{\min}^{\mathrm{F}}$ the departure time of the following train, and ε is the machine precision. In addition, we define binary variables $\delta_4(k) = \delta_1(k)\delta_2(k)$ and $\delta_5(k) = \delta_2(k)\delta_3(k)$ to deal with the nonlinear terms $\delta_1(k)\delta_2(k)$ and $\delta_2(k)\delta_3(k)$ in (34)-(35) respectively. According to the transformation properties in Section 2.2, the definitions of $\delta_4(k)$ and $\delta_5(k)$ are equivalent to linear constraints of the form (6). In addition, the auxiliary variables $z_i^{\mathrm{F}}(k)$ are introduced to deal with the nonlinear terms $\delta_i(k)v^{\mathrm{F}}(k)$, which is defined as

$$z_i^{\mathrm{F}}(k) = \delta_i(k)v^{\mathrm{F}}(k), \quad \text{for} \quad i = 1, 2, 3, 4, 5. \tag{37}$$

This definition is equivalent to linear constraints of the form (7). The constraints caused by the leading train in fixed block systems can thus be formulated into the MILP problem setting.

4.3. Optimal control problem for multiple trains under FBS systems

Now two solution approaches are proposed for the optimal control problem for multiple trains under FBS systems. For simplicity, we consider the optimal trajectory planning problem for two trains. However, the solution approaches can be easily extended to multiple trains. One is greedy (or sequential) approach, where the leading train's trajectory is first scheduled and then the trajectory of the following train is optimized based on the results of the leading train. The other approach is optimizing the trajectories of these two trains simultaneously.

In the greedy approach, first the trajectory of the leading train is determined by solving the MILP problem. Next, the optimal control problem of the following train is solved, which is similar to the one in Wang et al. (2011) both with the extra constraints of Section 4.2 caused by

the leading train in FBS system. The coefficient matrices in the mixed logical dynamic model (8)-(9) are determined by the following train. Since the trajectory of the leading train is known, $t^{\mathrm{L}}(l_{\ell(k)+i})$ is also known. Therefore, $\tilde{M}_i$ and $\tilde{m}_i$ are constants and (36) is then a system of linear constraints.

When optimizing the trajectories of multiple trains simultaneously, the models of these two trains are determined by a model of the form (8)-(9). The optimal control problem of these two successive trains can also be rewritten in the form of the MILP problem (11)-(12) but including the model and constraints of each train and the constraints caused by the FBS system. However, $t^{\mathrm{L}}(l_{\ell(k)+i})$ is now also a variable in this case since the leading train's trajectory also has to be optimized. The constraints (36) can be rewritten as

$$
\begin{aligned}
(T_{\mathrm{max}}^{\mathrm{F}} - t^{\mathrm{L}}(l_{\ell(k)+i}))\delta_i(k) &\leq -t^{\mathrm{F}}(k) + T_{\mathrm{max}}^{\mathrm{F}}, \\
(T_{\mathrm{min}}^{\mathrm{F}} - t^{\mathrm{L}}(l_{\ell(k)+i}) - \varepsilon)\delta_i(k) &\leq t^{\mathrm{F}}(k) - \varepsilon - t^{\mathrm{L}}(l_{\ell(k)+i}).
\end{aligned}
\tag{38}
$$

In order to deal with the nonlinear terms in (38), we define

$$
z_i^{\mathrm{L}}(k) = t^{\mathrm{L}}(l_{\ell(k)+i})\delta_i(k), \quad \text{for} \quad i = 1,2,3.
\tag{39}
$$

Similar to $z_i^{\mathrm{F}}(k)$, the auxiliary variables $z_i^{\mathrm{L}}(k)$ is equivalent to linear constraints according to the transformation properties in Section 2.2.

5. MBS system constraints and their formulation into the MILP approach

5.1. Discretizing the MBS constraints

Recall that the mixed logical dynamic model of the train's operation is discretized in space with N space intervals with grid points s_k, $k = 1, \ldots, N+1$ as shown in Section 2.3. Here, we discretize the constraint (15) caused by the MBS system at the grid points s_k as

$$
t^{\mathrm{F}}(k) \geq t^{\mathrm{L}}(k) + t_{\mathrm{r}}^{\mathrm{F}} + t_{\mathrm{b}}^{\mathrm{F}}(k) + t_{\mathrm{safe}}^{\mathrm{F}}(k), \quad \text{for} \quad k = 1,2,\ldots,N,
\tag{40}
$$

$$
t^{\mathrm{F}}(k) \geq t^{\mathrm{L}}(k) + t_{\mathrm{r}}^{\mathrm{F}} + t_{\mathrm{b,max}}^{\mathrm{F}} + t_{\mathrm{d}}^{\mathrm{L}} + t_{\mathrm{safe}}^{\mathrm{L}}, \quad \text{for} \quad k = N+1.
\tag{41}
$$

In addition, some intermediate constraints are introduced to ensure that the points between the grid points also satisfy the constraints caused by the MBS system. According to (15), we obtain the following constraint for each $s \in [s_k, s_{k+1}]$ as:

$$
t^{\mathrm{F}}(s) - t_{\mathrm{r}}^{\mathrm{F}} - t_{\mathrm{b}}^{\mathrm{F}}(s) - t_{\mathrm{safe}}^{\mathrm{F}}(s) \geq t^{\mathrm{L}}(s),
\tag{42}
$$

If we assume the left-hand side of (42) to be an affine function in the interval $[s_k, s_{k+1}]$, then we can add the following constraints:

$$
\begin{aligned}
(1-\alpha)(t^{\mathrm{F}}(k) - t_{\mathrm{r}}^{\mathrm{F}} - t_{\mathrm{b}}^{\mathrm{F}}(k) - t_{\mathrm{safe}}^{\mathrm{F}}(k)) &+ \alpha(t^{\mathrm{F}}(k+1) - t_{\mathrm{r}}^{\mathrm{F}} - t_{\mathrm{b}}^{\mathrm{F}}(k+1) - t_{\mathrm{safe}}^{\mathrm{F}}(k+1)) \\
&\geq t^{\mathrm{L}}(s + \alpha\Delta s_k),
\end{aligned}
\tag{43}
$$

for some values α in a finite subset $S_\alpha \in [0,1)$, e.g. $S_\alpha = \{0.1, 0.2, \ldots, 0.9\}$, where $t^{\mathrm{L}}(s + \alpha\Delta s_k)$ is known if the optimal trajectory of the leading train is fixed. Note that for $\alpha = 0$ and $\alpha = 1$ (40) is retrieved (except if $k = N-1$). However, if the leading train's trajectory is not known beforehand, then we need to optimize both trajectories simultaneously. In this case, the term $t^{\mathrm{L}}(s + \alpha\Delta s_k)$ is unknown. If we assume the right-hand side of (42) is also an affine function, i.e. $t^{\mathrm{L}}(s + \alpha\Delta s_k) = (1-\alpha)t^{\mathrm{L}}(k) + \alpha t^{\mathrm{L}}(k+1)$, then it is sufficient to check (42) in the points k and $k+1$ (i.e., for $\alpha = 0$ and $\alpha = 1$), since due to linearity (42) will then also automatically be satisfied for all intermediary points.

12

5.2. Considering the MBS constraints into the MILP approach

Note that the constraints (40), (41), and (43) are linear in $t^L(k)$, $t^L(k+1)$, $t^F(k)$. However, they are nonlinear in $v^F(k)$ and $v^F(k+1)$ since the time safety margin (17) is a nonlinear function of the following train's velocity $v^F(k)$. Furthermore, the kinetic energy per mass $E^F(k)$ is one of the states instead of $v^F(k)$ with $E^F(k) = 0.5(v^F(k))^2$ (cf. Section 2). Therefore, both the braking time $t_b^F(k)$ and the safe time margin $t_{\text{safe}}^F(k)$ are nonlinear functions of $E^F(k)$, where

$$t_b^F(k) = \frac{1}{a_b^F} \sqrt{2E^F(k)} \tag{44}$$

and

$$t_{\text{safe}}^F(k) = (S_{\text{SM}} + L_t^L) \frac{1}{\sqrt{2E^F(k)}}. \tag{45}$$

The nonlinear functions $f_1(\cdot) : E^F \to \sqrt{2E^F}$ and $f_2(\cdot) : E^F \to \frac{1}{\sqrt{2E^F}}$ could be approximated by PWA functions as follows. There are various methods for approximating functions in a PWA way, see e.g., the overview by Azuma et al. (2010). In this paper, we first select the number of regions of the PWA function based on the trade-off of complexity and accuracy. Next, the interval lengths and parameters of the affine functions is optimized using least-squares optimization for $f_1(\cdot)$. Then the parameters of the affine function for $f_2(\cdot)$ is optimized using the same number of regions and same interval lengths of the PWA approximations of $f_1(\cdot)$. If we consider approximations with 2 affine subfunctions, the PWA approximations of functions $f_1(\cdot)$ and $f_2(\cdot)$ can be written as

$$f_{1,\text{PWA}}(E^F(k)) = \begin{cases} \alpha_1 E^F(k) + \beta_1 & \text{for } E_{\min} \leq E^F(k) < E_1, \\ \alpha_2 E^F(k) + \beta_2 & \text{for } E_1 \leq E^F(k) \leq E_{\max}, \end{cases} \tag{46}$$

$$f_{2,\text{PWA}}(E^F(k)) = \begin{cases} \lambda_1 E^F(k) + \mu_1 & \text{for } E_{\min} \leq E^F(k) < E_1, \\ \lambda_2 E^F(k) + \mu_2 & \text{for } E_1 \leq E^F(k) \leq E_{\max}, \end{cases} \tag{47}$$

with optimized parameters α_1, α_2, β_1, β_2, λ_1, λ_2, μ_1, μ_2, and E_1. For more details of this transformation into PWA functions, see Wang et al. (2011). Now the constraint (40) can be approximated as the following linear constraint:

$$t^F(k) \geq t^L(k) + t_r^F + \frac{1}{a_b^F}(\alpha_1 E^F(k) + \beta_1) + (S_{\text{SM}} + L_t^L)(\lambda_1 E^F(k) + \mu_1), \quad \text{if} \quad E_{\min} \leq E^F(k) < E_1 \tag{48}$$

$$t^F(k) \geq t^L(k) + t_r^F + \frac{1}{a_b^F}(\alpha_2 E^F(k) + \beta_2) + (S_{\text{SM}} + L_t^L)(\lambda_2 E^F(k) + \mu_2), \quad \text{if} \quad E_1 \leq E^F(k) \leq E_{\max} \tag{49}$$

Similarly, the constraints (41) and (42) can also be written as linear constraints. These approximated linear constraints caused by the MBS system can be easily included in the MILP approach and we still get an MILP problem.

5.3. Optimal control problem for multiple trains under MBS systems

The greedy approach and the simultaneous approach mentioned in Section 4.3 can also be applied in MBS systems. In the greedy approach $t^L(k)$ and $t^L(s + \alpha \Delta s_k)$ are known for the trajectory planning problem for the following train since the trajectory of the leading train is known by the zone controller or the following train. The trajectory planning problem for the following train is similar to the one in Wang et al. (2011) but with the MBS constraints of Section

13

Table 1: Parameters of train and line path

Property	Symbol	Value
Train mass [kg]	m	$2.78 \cdot 10^5$
Basic resistance [N/kg]	R_b	$0.0142 + 1.0393 \cdot 10^{-4} v^2$
Mass factor	ρ	1.06
Maximum velocity [m/s]	V_{max}	22.2
Line length [m]	s_{end}	1332
Minimum kinetic energy [J]	E_{min}	0.1
Maximum traction force [N]	u_{max}	$2.224 \cdot 10^5$
Maximum braking force (regular) [N]	u_{min}	$-2.224 \cdot 10^5$

Table 2: Parameters for the calculation of the minimum headway

Property	Symbol	Value
Train length [m]	L_t	90
Safety margin [m]	S_{SM}	30
Length of the secure section [m]	L_s	60
Initial acceleration [m/s^2]	a_{acc}^L	1
Braking deceleration [m/s^2]	a_b^F	0.9
Braking reaction time [s]	t_r	1
Station dwell time [s]	t_d	25

5.2. When optimizing the trajectories of multiple trains at the same time, the model for each of these trains is determined by a model of the form (8)-(9). The optimal control problem of these successive trains can also be rewritten in the form of the MILP problem (11)-(12). However, the number of the state variables, binary variables, auxiliary variables, and constraints increase linearly with the number of trains compared to the case of a single train. Therefore, the size of this optimal trajectory planning problem is much bigger than the problem for a single train and the computation time of the bigger problem will be much longer. However, since optimizing the trajectories of two trains at the same time is a global optimization problem for these two trains, the control performance will in general be better than that of the greedy approach.

6. Case study

In order to demonstrate the performance of the proposed greedy and simultaneous approaches for the optimal trajectory planning for multiple trains under an FBS system and an MBS system, a part of the Beijing Yizhuang subway line is used as a test case study.

6.1. Set-up

The performance of the MILP approach is compared with the widely used pseudospectral method and for both approaches we consider both the greedy and the simultaneous variant. For the sake of simplicity, we only consider two[3] stations in the Yizhuang subway line: Songjiazhuang station and Xiaocun station. The track length between these two stations is 1332 m and

---

[3]Note however that the MILP approaches and the pseudospectral methods can also be applied if more than 2 stations are considered.
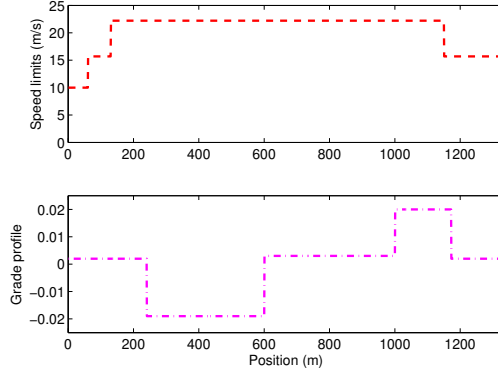
Figure 3: The speed limits and the grade profile between Songjiazhuang station and Xiaocun station

the speed limits and grade profile are shown in Figure 3. The parameters of the train and the line path are listed in Table 1. The rotating mass factor is often chosen as 1.06 in the literature (Hansen & Pachl, 2008) and therefore we also adopt this value. According to the assumptions made in Section 2.1, the unit kinetic energy should be larger than some positive threshold $E_{\min}$. In this test case, the minimum kinetic energy is chosen as 0.1 J. The maximum traction force of the train is a nonlinear function of the train's velocity and the maximum value of this function is 315 kN. Moreover, the maximum acceleration and maximum deceleration used for trajectory planning along the line is assumed to be 0.8 m/s^2 in order to make sure that the planned trajectory can be followed by the train controlled by the lower level controller. Since the train mass here is 2.78·10^5 kg, the maximum traction force and maximum braking force are 222.4 kN and -222.4 kN, respectively. The objective function of the optimal train control problem considered in this paper is the energy consumption of the train operation without regenerative braking (cf. (10)).

In this case study, two trains are scheduled to run from Songjiazhuang station with a headway of 75 s to Xiaocun station. We consider two cases: the FBS system and the MBS system. Moreover, we assume that the leading train has a malfunction during the whole simulation and as a consequence its maximum speed is reduced to 40 km/h, i.e. 11.1 m/s. In addition, the leading train and the following train will arrive to different platforms in Xiaocun station and the following train will overtake the leading train at Xiaocun station. The parameters for the calculation of the minimum headway are given in Table 2. The length of the train is 90 m and the reaction time of the driver is 1 s. For the FBS system, we assume that there exist four fixed block sections between Songjiazhuang station and Xiaocun station and all fixed block sections are of equal length, i.e. 333 m. The minimum headway of the FBS system can be calculated according to (13), which is equal to 98.4 s. Based on the parameters of Table 2, the run-in/run-out time $t_{\text{in}-\text{out}}$ in (18) is equal to 44.6 s and the minimum headway of the MBS system equals 69.6 s. Note that the headway 75 s is smaller than the minimum headway of the FBS system and is larger than the minimum headway of the MBS system.

In the MILP approaches, the lengths Δs_k of the intervals $[s_k, s_{k+1}]$ depend on the speed limits, gradient profile, fixed block length, and so on. If the number of the space intervals N is large, then the accuracy will be better but the computation time of the MILP approaches will be longer.

For this case study, the number of space intervals N is chosen as 20, 40, and 60, respectively. Moreover, the space intervals are taken to have equal length being 66.6 m, 33.3 m, and 22.2 m respectively for the different three values of N. In addition, the nonlinear terms in the trajectory planning problem, such as the nonlinear terms in the differential equations of the train model, are approximated by PWA functions (see Wang et al. (2013) for more details). If we take PWA approximations of the nonlinear terms with more subfunctions, the approximation accuracy will be better. Here, the PWA functions with 2 subfunctions and 3 subfunctions are compared. We use the CPLEX solver via the Tomlab[4] interface to Matlab for solving the MILP problems.

The pseudospectral method is a state-of-the-art method for solving optimal control problems (Elnagar et al., 1995; Gong et al., 2008). In the pseudospectral method, the state and control functions are approximated using orthogonal polynomials based on interpolation at orthogonal collocation points, such as the Gauss points. The differential equations of the optimal control problem can then be approximated by algebraic equations. The detailed information about the pseudospectral method is shown in Appendix B. The approximation error of the pseudospectral method can be reduced by taking more collocation points. The numbers of Gauss collocation points are taken as 20, 40, 80, and 120, respectively. There are several packages that implement the pseudospectral method (see Appendix B for detailed information). One of them is PROPT, which supports the description of the differential algebraic equations and can call many solvers, such as MINOS and SNOPT, to solve the resulting nonlinear programming problem. We in our case study use PROPT solver through the Tomlab interface to Matlab and SNOPT is used to solve the resulting nonlinear programming problem.

6.2. Results for the FBS system

Table 3 shows the performance of the MILP approaches and the pseudospectral methods for the trajectory planning of two trains in the FBS system. The performance mentioned here, such as the energy consumption and the end time violation, is calculated by applying the obtained optimal control inputs into the nonlinear train model (1). The total energy consumption is the sum of the energy consumption of the leading train and the following train. The end time violation is the sum of the absolute values of the differences between the real running times and the planned running times of the leading train and the following train. The energy consumption for each train is influenced by the sign of the difference between the real running time and the planned running time. If the real running time is larger than the planned running time, e.g. 105 s for the following train, then the energy consumption usually becomes less since a train can run with a smaller average speed. The CPU time is the sum of the time used to solve the optimal control problem

---

[4]Tomlab website: http://tomopt.com.

[5]For the greedy and simultaneous MILP approaches, the n in the notation n/m is the number of subfunctions used in the PWA approximations of the nonlinear terms in the differential equations of the nonlinear train model and m is the number of the discrete space intervals. For the greedy and simultaneous pseudospectral methods, the n indicates the number of collocation points used.

[6]For all four approaches, the number n_1 in the notation $n_1/n_2/n_3$ is the number of real-valued variables, n_2 is the number of integer-valued variables, and n_3 is the number of constraints. Note that for the greedy and simultaneous MILP approach, all the constraints are linear. Furthermore, in the greedy MILP and greedy pseudospectral methods, two subproblems are solved. One is for the trajectory planning problem of the leading train, the size of which is shown as L: $n_1/n_2/n_3$. The other is for the trajectory planning problem for the following train considering the constraints caused by the leading train, the size of which is shown as F: $n_1/n_2/n_3$. For the simultaneous MILP and simultaneous pseudospectral approaches, the trajectories of the leading train and the following train are obtained by solving a combined optimization problem.

Table 3: Performance comparison of the greedy and simultaneous approach using the MILP and pseudospectral method for the FBS system

| Approach	Method	Variant [5]	Problem size [6]	Total energy consumption [MJ]	Total end time violation [s]	Total CPU time [s]
Greedy	MILP	2/20	L: 99/40/462 F: 199/140/1116	114.48	3.17	1.34
		2/40	L: 199/80/922 F: 399/280/2326	113.77	1.95	14.22
		2/60	L: 299/120/1382 F: 599/420/3486	110.60	1.48	24.26
		3/20	L: 179/120/962 F: 279/220/1686	114.79	2.82	6.87
		3/40	L: 359/240/1542 F: 559/440/3366	112.58	2.21	96.56
		3/60	L: 539/360/2702 F: 839/660/5046	110.03	1.41	229.72
	Pseudo-spectral	20	L: 60/0/1107 F: 60/0/1307	112.59	2.52	231.83
		40	L: 120/0/1207 F: 120/0/1607	110.04	1.43	1381.71
		80	L: 240/0/1407 F: 240/0/2207	109.48	0.76	1935.09
		120	L: 360/0/1607 F: 360/0/2807	109.17	0.45	3588.10
Simul-taneous	MILP	2/20	358/180/1837	109.65	4.07	2.76
		2/40	718/360/3697	108.06	2.91	78.40
		2/60	1078/540/5557	106.32	1.65	204.38
		3/20	518/340/2877	108.44	3.19	24.13
		3/40	1038/680/5777	106.58	1.73	184.76
		3/60	1558/1020/8677	106.19	1.08	349.31
	Pseudo-spectral	20	120/0/2414	109.53	3.58	445.52
		40	240/0/2814	106.44	1.68	1521.30
		80	480/0/3614	105.92	0.78	3005.71
		120	720/0/4414	105.68	0.54	4875.23

17
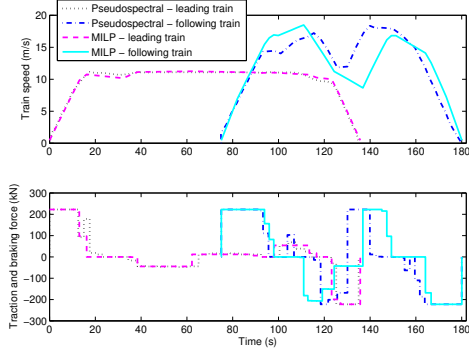
Figure 4: Trajectory planning for two trains under the FBS system with headway 75 s using the greedy MILP and pseudospectral approach
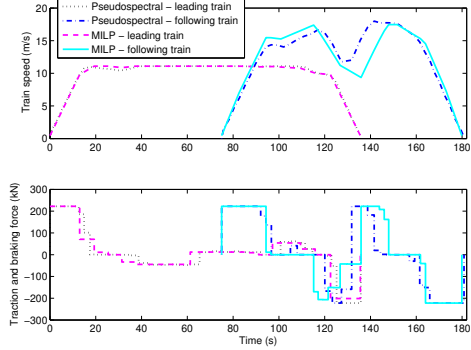
Figure 5: Trajectory planning for two trains under the FBS system with headway 75 s using the simultaneous MILP and pseudospectral approaches

for the leading train and the optimal control problem for the following train in greedy approach. In the simultaneous approach, the total CPU time is equal to the time spent by solving the optimal control problem since the optimal control inputs for the leading train and the following train are obtained simultaneously.

Furthermore, Figure 4 and Figure 5 show the optimal control inputs and the speed-position trajectories obtained by the MILP approaches and the pseudospectral methods for the FBS system, where the number of space intervals for the MILP approaches and the number of the collocation points for the pseudospectral methods are taken as 40 and the nonlinear terms in the nonlinear train model are approximated using PWA functions with 3 affine subfunctions for the MILP approach. The speed-position trajectories of the leading train and the following train were produced by applying the optimal control inputs obtained by solving the optimal control problems to the nonlinear train model. It is observed from Figure 4 and Figure 5 that the operation of the following train is affected by the leading train in the FBS system, where the signal at position 666 m shows a yellow aspect to the following train. Because the headway between the leading train and the following train is taken as 75 s, which is less than the minimum headway of the FBS system, i.e. 98.4 s. Thus, the following train must slow down to satisfy the speed limit caused by the yellow signal aspect, which is 40 km/h, i.e. 11.1 m/s.

In Figure 4, the corresponding energy consumption, the end time violation, and the computation time of the greedy MILP approach are 112.58 MJ, 2.21 s, and 96.56 s, respectively. For the greedy pseudospectral method, the energy consumption, the end time violation, and the calculation time of both trains are 110.04 MJ, 1.43 s, and 1381.71 s, respectively. It can be seen that the energy consumption and the end time violation of the greedy MILP approach are a bit larger than those of the greed pseudospectral method. However, the computation time of the greedy pseudospectral method is more than one order of magnitude longer than that of the greedy MILP approach.

The energy consumption, end time violation, and calculation time are 106.58 MJ, 1.73 s, 184.76 s, respectively, using the simultaneous MILP approach as shown in Figure 5. For the simultaneous pseudospectral method, they are 106.44 MJ, 1.68 s, 1521.30 s, respectively. When compared with the greedy MILP approach, the energy consumption and the end time violation
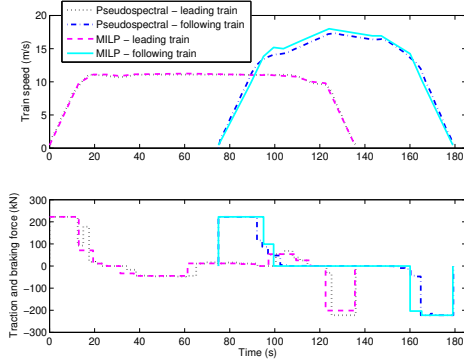
18

Figure 6: Trajectory planning for two trains under the MBS system with headway 75 s using the greedy MILP and pseudospectral approaches
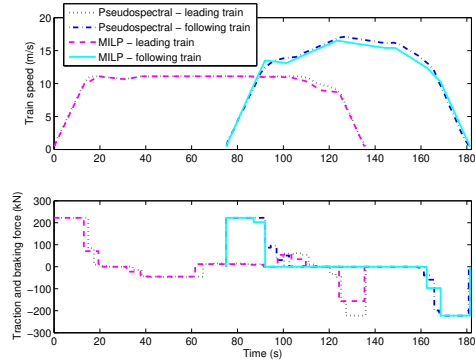
Figure 7: Trajectory planning for two trains under MBS system with headway 75 s using the simultaneous MILP and pseudospectral approaches

of the simultaneous MILP approach become smaller. Because the trajectories of the leading train and the following train are optimized simultaneously, which should be with better control performance theoretically since the leading train's trajectory can also be optimized with respect to the following train. However, the computation time of the simultaneous MILP approach becomes longer than the greedy MILP approach because in the simultaneous MILP approach, the size of the optimization problem is almost doubled. When comparing the simultaneous pseudospectral method with the greedy pseudospectral method, the similar observations as the MILP approach can be obtained.

As can be observed in Table 3, the energy consumption and the end time violation of the greedy MILP approach are generally larger than that of the greedy pseudospectral method with respect to the same number of discrete intervals and collocation points. However, the computation time of the greedy pseudospectral method is one to two orders of magnitude higher than that of the greedy MILP approach. In addition, the energy consumption and the end time violation become less if we take more discrete space intervals for the greedy MILP approach and more collocation points for the greedy pseudospectral method. The results obtained for the greedy MILP approach and the greedy pseudospectral method also hold for the simultaneous MILP approach and the simultaneous pseudospectral method. Moreover, it can be observed that the energy consumption of the simultaneous MILP approach is less than that of the greedy MILP approach, while the computation times of the simultaneous MILP approach are higher than those of the greedy MILP approach. This also holds for the greedy and simultaneous pseudospectral method.

6.3. Results for the MBS system

The performance of the greedy and simultaneous approaches is shown in Table 4 for the MBS system. In particular, Figure 6 and Figure 7 show the speed-position trajectories and the optimal control inputs for the MBS system with the same set-up as the case illustrated in Figure 4 and Figure 5. Similarly, the speed-position trajectories, the end time violation, etc. are obtained by applying the optimal control inputs to the nonlinear train model (1). As we can see from Figure 6 and Figure 7, the operation of the following train is not affected by the leading train since the scheduled headway 75 s is larger than the minimum headway of the MBS system 69.6 s.

19

Table 4: Performance comparison of the greedy and simultaneous approach using the MILP and pseudospectral method for the MBS system

Approach	Method	Variant	Problem size	Total energy consumption [MJ]	Total end time violation [s]	Total CPU time [s]
Greedy	MILP	2/20	L: 99/40/462 F: 99/40/632	69.16	3.45	1.41
		2/40	L: 199/80/922 F: 199/80/1292	68.34	2.47	12.03
		2/60	L: 299/120/1382 F: 299/120/1952	67.56	1.08	24.19
		3/20	L: 179/120/962 F: 179/120/1152	68.76	2.79	9.87
		3/40	L: 359/240/1542 F: 359/240/2332	67.89	1.68	75.98
		3/60	L: 539/360/2702 F: 539/360/3662	67.12	1.34	254.80
	Pseudo-spectral	20	L: 60/0/1107 F: 60/0/1157	68.88	3.94	89.71
		40	L: 120/0/1207 F: 120/0/1257	67.42	1.66	729.24
		80	L: 240/0/1407 F: 240/0/1457	67.03	0.75	1483.42
		120	L: 360/0/1607 F: 360/0/1657	66.85	0.29	4542.20
Simul-taneous	MILP	2/20	198/80/1094	68.14	2.58	2.45
		2/40	398/160/2214	67.52	1.53	56.17
		2/60	598/240/3334	66.62	1.26	150.67
		3/20	358/240/2134	67.73	1.71	13.49
		3/40	718/480/4294	67.03	1.04	121.29
		3/60	1078/720/6454	66.87	0.85	420.37
	Pseudo-spectral	20	120/0/2264	68.62	3.61	161.15
		40	240/0/2464	67.50	1.37	1051.06
		80	480/0/2864	67.07	0.66	2984.23
		120	720/0/3264	66.26	0.31	6954.37

With respect to Figure 6, the energy consumption, the end time violation, and the computation time for the greedy MILP approach are 67.89 MJ, 1.68 s, and 75.98 s. In addition, the energy consumption, the end time violation, and the computation time for the greedy pseudospectral method are 67.42 MJ, 1.66 s, and 729.24 s. The energy consumption and the end time violation of the greedy MILP approach are slightly larger than those of the greedy pseudospectral method. However, the computation time of the greedy pseudospectral method is almost one order of magnitude larger than that of the greedy MILP approach. This also holds for the results obtained by the simultaneous MILP and pseudospectral approach. Generally, the total energy consumption and the total end time violation decrease with the increase of the number of the discrete space intervals in MILP approach and the number of collocation points in pseudospectral method. Nevertheless, the total CPU time increases quickly with respect to the number of the discrete space intervals and collocation points. For the greedy and/or simultaneous MILP approach, if we take the PWA approximations with more subfunctions, the end time violation also declines. Furthermore, when compared with the greedy MILP (or pseudospectral) approach, the simultaneous MILP (or pseudospectral) approach has better control performance in principle but it is with a much higher computation burden since the size of the optimization problem is almost doubled.

6.4. Discussion

The above simulation results show that when compared with the greedy pseudospectral method, the energy consumption and the end time violation of the greedy MILP approach are inconsiderably larger, but the computation time is one to two orders of magnitude shorter. Similarly, the energy consumption and the end time violation of the simultaneous MILP approach are lightly larger than these of the simultaneous pseudospectral method. However, the computation time of the simultaneous MILP approach is much shorter than that of the simultaneous pseudospectral method. Moreover, the energy consumption of the greedy MILP approach is larger than that of the simultaneous MILP approach, but the calculation time of the simultaneous MILP approach is longer in general. Furthermore, the same trends also hold for the energy consumption and the calculation time of the greedy pseudospectral method and the simultaneous pseudospectral method.

7. Conclusions and Future Work

In this paper, we have proposed two approaches, namely the greedy approach and simultaneous approach, to solve the optimal trajectory planning problem for multiple trains. In the greedy approach, the optimal trajectory planning problem of the leading train is solved first and then based on the optimal control inputs of the leading train, the trajectory planning problem for the following train is solved. For the simultaneous approach, the trajectories of the leading train and the following train are optimized at the same time. The constraints caused by the leading train in a fixed block signaling system and a moving block signaling system are included in the optimal trajectory planning problem for multiple trains. The nonlinear terms in the train model and constraints are approximated by piecewise affine functions. In this way, the optimal trajectory planning problem for multiple trains can then be recast as a mixed integer linear programming (MILP) problem. Furthermore, the performance of the greedy and the simultaneous MILP approach is compared with the greedy and the simultaneous pseudospectral method in a case study. The simulation results show that the MILP approaches have a similar control performance as the pseudospectral methods but they require a much less computation time.

A topic for future work will be an extensive comparison and assessment between the MILP approach, the pseudospectral method (also using other nonlinear programming subsolvers, e.g., MINOS and KNITRO), a dynamic programming algorithm (Hellström et al., 2010), and other approaches and frameworks (such as AMPL, APMonitor, and ASCEND) described in the literature for various case studies and a wide range of scenarios.

Appendix A. The relationship among position, speed, and acceleration

In this appendix the relationship among position, speed, and acceleration of a train based on a constant acceleration model is deduced explicitly. It is assumed that the initial position, speed, and time are s_0, v_0, and t_0, respectively. Similarly, s_e, v_e, and t_e are the end position, speed, and time, respectively.

Assuming a constant acceleration a during the time interval $[t_0, t_e]$, the relationship between the initial speed v_0 and the end speed v_e is

$$v_e = v_0 + a(t_e - t_0), \tag{A.1}$$

In addition, we have

$$s_e = s_0 + v_0(t_e - t_0) + \frac{1}{2}a(t_e - t_0)^2, \tag{A.2}$$

By substituting (A.1) into (A.2), we obtain

$$s_e = s_0 + v_0\frac{v_e - v_0}{a} + \frac{1}{2}a\frac{(v_e - v_0)^2}{a^2}, \tag{A.3}$$

which yields

$$2a(s_e - s_0) = v_e^2 - v_0^2. \tag{A.4}$$

So if v_0 is equal to 0, then we have

$$t_e - t_0 = \sqrt{\frac{2(s_e - s_0)}{a}}. \tag{A.5}$$

Appendix B. A general formulation of the pseudospectral method

The optimal train trajectory planning problem can be formulated as a multiple phase optimal control problem and then can be solved by the pseudospectral method. Below we describe a general optimal control problem with multiple phases and the solution procedure of the general optimal control problem using the pseudospectral method. This explanation is based on Ross & Fahroo (2004); Gong et al. (2008); Canuto et al. (1988); Elnagar et al. (1995); and Becerra (2010).

Appendix B.1. The multiple-phase optimal control problem

The general optimal control problem with N_p phases is formulated as follows (Ross & Fahroo, 2004). The objective function is

$$J = \sum_{i=1}^{N_p} \left(\varphi^{(i)}\big(x^{(i)}(t_f^{(i)}), p^{(i)}, t_f^{(i)}\big) + \int_{t_0^{(i)}}^{t_f^{(i)}} L^{(i)}\big(x^{(i)}(t), u^{(i)}(t), p^{(i)}, t\big)\mathrm{d}t \right), \tag{B.1}$$

where $[t_0^{(i)}, t_f^{(i)}]$ is the time interval for the ith phase, $u^{(i)}(\cdot)$ and $x^{(i)}(\cdot)$ are the control trajectories and state trajectories, $p^{(i)}$ are the static parameters, for $i = 1, 2, \ldots, N_p$. The objective function (B.1) is subject to the differential constraints

$$\dot{x}^{(i)}(t) = f^{(i)}\big(x^{(i)}(t), u^{(i)}(t), p^{(i)}, t\big), \quad t \in [t_0^{(i)}, t_f^{(i)}], \tag{B.2}$$

the path constraints

$$h_L^{(i)} \leq h^{(i)}\big(x^{(i)}(t), u^{(i)}(t), p^{(i)}, t\big) \leq h_U^{(i)}, \quad t \in [t_0^{(i)}, t_f^{(i)}], \tag{B.3}$$

the event constraints

$$e_L^{(i)} \leq e^{(i)}\big(x^{(i)}(t_0^{(i)}), u^{(i)}(t_0^{(i)}), x^{(i)}(t_f^{(i)}), u^{(i)}(t_f^{(i)}), p^{(i)}, t_0^{(i)}, t_f^{(i)}\big) \leq e_U^{(i)}, \quad t \in [t_0^{(i)}, t_f^{(i)}], \tag{B.4}$$

the linkage constraints

$$
\begin{aligned}
\Psi_L \leq \Psi\big(& x^{(1)}(t_0^{(1)}), u^{(1)}(t_0^{(1)}), x^{(1)}(t_f^{(1)}), u^{(1)}(t_f^{(1)}), p^{(1)}, t_0^{(1)}, t_f^{(1)}, \\
& x^{(2)}(t_0^{(2)}), u^{(2)}(t_0^{(2)}), x^{(2)}(t_f^{(2)}), u^{(2)}(t_f^{(2)}), p^{(2)}, t_0^{(2)}, t_f^{(2)}, \\
& \ldots \\
& x^{(N_p)}(t_0^{(N_p)}), u^{(N_p)}(t_0^{(N_p)}), x^{(N_p)}(t_f^{(N_p)}), u^{(N_p)}(t_f^{(N_p)}), p^{(N_p)}, t_0^{(N_p)}, t_f^{(N_p)}\big) \leq \Psi_U,
\end{aligned}
\tag{B.5}
$$

the bound constraints

$$
\begin{aligned}
u_L^{(i)} \leq u^{(i)}(t) \leq u_U^{(i)}, \quad & x_L^{(i)} \leq x^{(i)}(t) \leq x_U^{(i)}, \quad t \in [t_0^{(i)}, t_f^{(i)}], \\
p_L^{(i)} \leq p^{(i)} \leq p_U^{(i)}, \quad & \underline{t}_0^{(i)} \leq t_0^{(i)} \leq \bar{t}_0^{(i)}, \quad \underline{t}_f^{(i)} \leq t_f^{(i)} \leq \bar{t}_f^{(i)},
\end{aligned}
\tag{B.6}
$$

and the following constraints

$$t_f^{(i)} - t_0^{(i)} \geq 0. \tag{B.7}$$

Appendix B.2. The solution process of the optimal control problem

Let $i \in \{1, 2, \ldots, N_p\}$ be a particular phase of the optimal control problem (B.1)-(B.7) and let $(\cdot)^{(i)}$ denote information for the ith phase. The ith phase of the optimal control problem can be transformed from the interval $t \in [t_0^{(i)}, t_f^{(i)}]$ to the interval $\tau \in [-1, 1]$ for $i = 1, 2, \ldots, N_p$ by introducing the transformation (Ross & Fahroo, 2004):

$$\tau = \frac{2}{t_f^{(i)} - t_0^{(i)}} t - \frac{t_f^{(i)} + t_0^{(i)}}{t_f^{(i)} - t_0^{(i)}}. \tag{B.8}$$

Now we approximate the state and control functions using Legendre pseudospectral approximation. The state $x_k^{(i)}(\tau)$, $\tau \in [-1, 1]$ is approximated by the N_ith order Lagrange polynomial $x_k^{N_i,(i)}(\tau)$ based on interpolation at the Legendre-Gauss-Lobatto (LGL) points (Canuto et al., 1988)

$$x_k^{(i)}(\tau) \approx x_k^{N_i,(i)}(\tau) = \sum_{n=0}^{N_i} \bar{x}_k^{N_i,(i)}(\tau_n) \phi_n^{(i)}(\tau), \tag{B.9}$$

23

where $\bar{x}_k^{N_i,(i)}(\tau_n)$ is a discrete approximation of the LGL point τ_n and the Lagrange basis polynomials $\phi_n^{(i)}(\tau)$ for $n = 0, 1, \cdots, N_i$ are defined as

$$\phi_n^{(i)}(\tau) = \prod_{m=0, m \neq n}^{N_i} \frac{\tau - \tau_m^{(i)}}{\tau_n^{(i)} - \tau_m^{(i)}}, \tag{B.10}$$

and $\tau_n^{(i)}$ for $n = 0, 1, \ldots, N_i$ are the LGL points, which are defined as $\tau_0^{(i)} = -1$, $\tau_{N_i}^{(i)} = 1$, and τ_n being the roots of the derivative of the Legendre polynomial

$$L_{N_i}(\tau) = \frac{1}{2^{N_i} N_i!} \frac{\mathrm{d}^{N_i}}{\mathrm{d}\tau^{N_i}} (\tau^2 - 1)^{N_i},$$

in the interval $[-1, 1]$ for $n = 1, 2, \ldots, N_i - 1$. The control $u^{(i)}(\tau)$ can be approximated in a similar way. The derivative of $x_k^{N_i,(i)}(\tau)$ at the LGL points τ_n can be obtained by differentiating (B.9), which can be expressed as a matrix multiplication as follows:

$$\dot{x}_k^{(i)}(\tau_n) \approx \dot{x}_k^{N_i,(i)}(\tau_n) = \sum_{j=0}^{N_i} \tilde{D}_{nj}^{(i)} \bar{x}_k^{N_i,(i)}(\tau_j), \tag{B.11}$$

where $\tilde{D}^{(i)}$ is the $(N_i + 1) \times (N_i + 1)$ differential approximation matrix (Gong et al., 2007) given by

$$\tilde{D}_{nj}^{(i)} = \begin{cases} \frac{\phi_{N_i}^{(i)}(\tau_n)}{\phi_{N_i}^{(i)}(\tau_j)} \frac{1}{\tau_n - \tau_j}, & \text{if } n \neq j, \\ -N_i(N_i + 1)/4, & \text{if } n = j = 0, \\ N_i(N_i + 1)/4, & \text{if } n = j = N_i, \\ 0, & \text{otherwise.} \end{cases} \tag{B.12}$$

The differential constraints can be recast into algebraic constraints via the differential approximation matrix. In addition, the path constraints (B.3) can be discretized at the LGL points. Note that the dynamic constraints and path constraints are only collocated at the LGL points, which means both the dynamic and path constraints might be violated in between collocation points (Rutquist & Edvall, 2008). The objective function (B.1) can be approximated using LGL points as

$$\begin{aligned} J = \sum_{i=1}^{N_p} & \left(\varphi^{(i)} \left(\bar{x}^{N_i,(i)}(-1), \bar{x}^{N_i,(i)}(1), p^{(i)}, t_0^{(i)}, t_f^{(i)} \right) \right. \\ & \left. + \frac{t_f^{(i)} - t_0^{(i)}}{2} \sum_{n=0}^{N_i} L^{(i)} \left(\bar{x}^{N_i,(i)}(\tau_n), \bar{u}^{N_i,(i)}(\tau_n), p^{(i)}, \tau_n \right) \omega_n \right), \end{aligned} \tag{B.13}$$

where ω_n are the weights given by

$$\omega_n = \frac{2}{N(N+1)} \frac{1}{(L_{N_i}(\tau_n))^2}, \quad \text{for } n = 0, 1, \ldots, N_i. \tag{B.14}$$

If we include all the decision variables in vector y, the optimal control problem is then ready to be expressed as a nonlinear programming problem:

$$\min_{y} J(y) \tag{B.15}$$

24

subject to

$$G_L \leq G(y) \leq G_U$$
$$y_L \leq y \leq y_U. \tag{B.16}$$

By defining $G(y)$, G_L, G_U, y_L, and y_U properly, we can write all constraints in the form (B.16).

There exist several commercial and free packages that implement the pseudospectral method: SOCS (Betts, 2002) and DIRCOL (von Stryk, 1999) are Fortran-based proprietary packages, while PROPT (Rutquist & Edvall, 2008) and DIDO (Ross, 2004) are examples of commercial softwares with Matlab interface. A Matlab-based open source tool that uses the Gauss pseudospectral method is GPOPS (Rao et al., 2010). PSOPT is an open source optimal control package written in C++, including Legendre and Chebyshev pseudospectral discretizations (Becerra, 2010).

Acknowledgments

References

References

Atamtürk, A., & Savelsbergh, M. W. P. (2005). Integer-programming software systems. *Annals of Operations Research*, *140*, 67–124.

Azuma, S. I., Imura, J. I., & Sugie, T. (2010). Lebesgue piecewise affine approximation of nonlinear systems. *Nonlinear Analysis: Hybrid Systems*, *4*, 92–102.

Becerra, V. M. (2010). Solving complex optimal control problems at no cost with PSOPT. In *Proceedings of IEEE Multi-Conference on Systems and Control* (pp. 1391–1396). Yokohama, Japan.

Bemporad, A., & Morari, M. (1999). Control of systems integrating logic, dynamics, and constraints. *Automatica*, *35*, 407–427.

Betts, J. T. (2002). A direct approach to solving optimal control problems. *Computing in Science & Engineering*, *1*, 73–75.

Canuto, C., Hussaini, M. Y., Quarteroni, A., & Zang, T. (1988). *Spectral Methods in Fluid Dynamics*. New York: Springer Verlag.

Chang, C., & Sim, S. (1997). Optimising train movements through coast control using genetic algorithms. *IEE Proceedings - Electric Power Applications*, *144*, 65–73.

Chang, C., & Xu, D. (2000). Differential evolution based tunning of fuzzy automatic train operation for mass rapid transit system. *IEE Proceedings - Electric Power Applications*, *147*, 206–212.

Ding, Y., Bai, Y., Liu, F., & Mao, B. (2009). Simulation algorithm for energy-efficient train control under moving block system. In *Proceedings of the 2009 World Congress on Computer Science and Information Engineering* (pp. 498–502). Los Angeles, USA.

Elnagar, G., Kazemi, M. A., & Razzaghi, M. (1995). The pseudospectral legendre method for discretizing optimal control problems. *IEEE Transactions on Automatic Control*, *40*, 1793–1796.

Franke, R., Meyer, M., & Terwiesch, P. (2002). Optimal control of the driving of trains. *Automatisierungstechnik*, *50*, 606–614.

Franke, R., Terwiesch, P., & Meyer, M. (2003). An algorithm for the optimal control of the driving of trains. In *Proceedings of the 39th IEEE Conference on Decision and Control* (pp. 2123–2128). Sydney, Australia.

Gong, Q., Kang, W., Bedrossian, N., Fahroo, F., P.Sekhavat, & Bollino, K. (2007). Pseudospectral optimal control for military and industrial applications. In *Proceedings of the 46th IEEE Conference on Decision and Control* (pp. 4128–4142). New Orleans, LA, USA.

Gong, Q., Ross, I. M., Kang, W., & Fahroo, F. (2008). Connections between the covector mapping theorem and convergence of pseudospectral methods for optimal control. *Computational optimization and applications*, *41*, 307–335.

Gu, Q., Lu, X., & Tang, T. (2011). Energy saving for automatic train control in moving block signaling system. In *Proceedings of the 14th International IEEE Conference on Intelligent Transportation Systems* (pp. 1305–1310). Washington, DC, USA.

Han, S. H., Byen, Y. S., Baek, J. H., An, T. K., Lee, S. G., & Park, H. J. (1999). An optimal automatic train operation (ATO) control using genetic algorithms (GA). In *Proceedings of the IEEE Region 10 Conference (TENCON 99)* (pp. 360–362). Cheju Island, South Korea volume 1.

Hansen, I., & Pachl, J. (2008). *Railway, Timetable & Traffic: Analysis, Modelling, Simulation*. Hamburg, Germany: Eurailpress.

Hellström, E., slund, J. A., & Nielsen, L. (2010). Design of an efficient algorithm for fuel-optimal look-ahead control. *Control Engineering Practice*, *18*, 1318–1327.

Hill, R. J., & Bond, L. J. (1995). Modeling moving block railway signaling system using discrete-event simulations. In *Proceedings of the 1995 IEEE/ASME Joint Railroad Conference* (pp. 105–111). Baltimore, MD, USA.

Howlett, P. (2000). The optimal control of a train. *Annals of Operations Research*, *98*, 65–87.

Howlett, P., Milroy, I., & Pudney, P. (1994). Energy-efficient train control. *Control Engineering Practice*, *2*, 193–200.

Howlett, P. G., & Pudney, P. J. (1995). *Energy-Efficient Train Control*. London, UK: Advances in Industrial Control. Springer-Verlag.

Ke, B. R., Lin, C. L., & Lai, C. W. (2011). Optimization of train-speed trajectory and control for mass rapid transit systems. *Control Engineering Practice*, *19*, 675–687.

Khmelnitsky, E. (2000). On an optimal control problem of train operation. *IEEE Transactions on Automatic Control*, *45*, 1257–1266.

Ko, H., Koseki, T., & Miyatake, M. (2004). Application of dynamic programming to optimization of running profile of a train. In *Computers in Railways IX, WIT Press* (pp. 103–112). Southhampton, Boston, USA volume 15.

Linderoth, J. T., & Ralphs, T. K. (2005). Noncommercial software for mixed-integer linear programming. In J. K. Karlof (Ed.), *Integer Programming: Theory and Practice* (pp. 253–303). Wilmington, USA: CRC Press Operations Research Series.

Liu, R., & Golovicher, I. M. (2003). Energy-efficient operation of rail vehicles. *Transportation Research Part A: Policy and Practice*, *37*, 917–931.

Lu, Q., & Feng, X. (2011). Optimal control strategy for energy saving in trains under the four-aspected fixed auto block system. *Journal of Modern Transportation*, *19*, 82–87.

Pachl, J. (2009). *Railway Operation and Control Second Edition*. Centralia WA,US: Gorham Printing.

Pearson, L. (1973). *Moving Block Signalling*. Loughborough University of Technology, England: Ph.D. thesis.

Peng, H. (2008). *Urban Rail Transit System*. Beijing, China: China Communication Press.

Rao, A. V., Benson, D. A., Darby, C., Patterson, M. A., Francolin, C., & Sanders, I. (2010). Algorithm 902: GPOPS, a matlab software for solving multiple-phase optimal control problems using the Gauss pseudospectral method. *ACM Transactions on Mathematical Software*, *37*, 22:1–22:39.

Ross, I. M. (2004). *User's manual for DIDO: A MATLAB application package for solving optimal control problems*. Pullman, US: Tomlab Optimization Inc.

Ross, I. M., & Fahroo, F. (2004). Pseudospectral knotting methods for solving optimal control problems. *Journal of Guidance, Control, and Dynamics*, *27*, 397–405.

Rutquist, P., & Edvall, M. (2008). *PROPT: MATLAB Optimal Control Software*. Pullman, US: Tomlab Optimization Inc.

von Stryk, O. (1999). *User's Guide for DIRCOL (Version 2.1): A Direct Collocation Method for the Numerical Solution of Optimal Control Problems*. Technical Report Technische Universität Darmstadt Germany.

Takeuchi, H., Goodman, C., & Sone, S. (2003). Moving block signaling dynamics: performance measures and re-starting queued electric trains. *IEE Proceedings - Electric Power Applications*, *150*, 483–492.

Vašak, M., Baotić, M., Perić, N., & Bago, M. (2009). Optimal rail route energy management under constraints and fixed arrival time. In *Proceedings of the European Control Conference* (pp. 2972–2977). Budapest, Hungary.

Wang, Y., De Schutter, B., van den Boom, T., & Ning, B. (2013). Optimal trajectory planning for trains – A pseudospectral method and a mixed integer linear programming approach. *Transportation Research Part C*, *29*, 97–114.

Wang, Y., De Schutter, B., Ning, B., Groot, N., & van den Boom, T. (2011). Optimal trajectory planning for trains using mixed integer linear programming. In *Proceedings of the 14th International IEEE Conference on Intelligent Transportation Systems (ITSC 2011)* (pp. 1598–1604). Washington, DC, USA.

Williams, H. P. (1999). *Model Building in Mathematical Programming (4th ed.)*. Chichester, England: John Wiley & Sons.